Enhancing the Anion–Transport Selectivity of Multilayer Polyelectrolyte Membranes by Templating with Cu2+

3 AUTHORS, INCLUDING:

Anagi M Balachandra
Technova Corporation

32 PUBLICATIONS   **235** CITATIONS

Enhancing the Anion-Transport Selectivity of Multilayer Polyelectrolyte Membranes by Templating with Cu²⁺

Anagi M. Balachandra, Jinhua Dai, and Merlin L. Bruening*

Department of Chemistry, Michigan State University, East Lansing, Michigan 48824

Received September 17, 2001; Revised Manuscript Received January 15, 2002

ABSTRACT: Alternating deposition of oppositely charged polyelectrolytes on porous supports is an attractive way to synthesize selective, ultrathin ion-separation membranes. This study reports the use of Cu²⁺ as a template in poly(acrylic acid) (PAA)/poly(allylamine hydrochloride) (PAH) membranes to control fixed charge density and hence enhance anion-transport selectivity. Alternating deposition of PAA partially complexed with Cu²⁺ and PAH on porous alumina supports followed by removal of Cu²⁺ and deprotonation results in fixed −COO⁻ sites in these films. Cu²⁺-templated PAA/PAH membranes show a 4-fold increase in Cl⁻/SO₄²⁻ transport selectivity compared to pure PAA/PAH membranes deposited under similar conditions. Cross-linking of these templated membranes further increases Cl⁻/SO₄²⁻ selectivity by an order of magnitude to a value of 610. Changing the top layer of cross-linked, Cu²⁺-templated membranes from negatively charged PAA to positively charged PAH decreases Cl⁻/SO₄²⁻ selectivity 10-fold, indicating that Donnan repulsion from a negatively charged surface is a major factor behind selectivity. Modeling studies suggest that selectivity is due to both Donnan exclusion and diffusivity differences among ions.

Introduction

Alternating layer-by-layer adsorption of polyanions and polycations is an attractive method for forming ultrathin separation membranes because of its versatility and simplicity.[1,2] Previous studies of multilayer polyelectrolyte membranes (MPMs) deposited on porous supports showed selective separation of monovalent and divalent ions,[3−5] modest gas separations[3,6−9] and highly selective pervaporation.[3,9−12] In the preceding paper,[13] we utilized derivatization of poly(acrylic acid) (PAA) or poly(allylamine hydrochloride) (PAH) to vary the fixed charge in MPMs and control ion-transport selectivity. This study focuses on enhancing the anion-transport selectivities of MPMs by increasing their fixed negative charge density through templating with Cu²⁺. Introduction of ion-exchange sites occurs due to partial Cu²⁺ complexation of the carboxylate groups of PAA during the deposition of PAA/PAH membranes. Removal of Cu²⁺ in acidic solution and subsequent deprotonation of −COOH groups yields fixed −COO⁻ ion-exchange sites as shown in Figure 1. Studies of ion transport through Cu²⁺-templated poly(acrylic acid) (PAA-Cu)/PAH membranes show a 4-fold increase in Cl⁻/SO₄²⁻ selectivities compared to pure PAA/PAH membranes deposited at similar conditions. Cross-linking[14,15] of templated films through heat-induced amidation can yield Cl⁻/SO₄²⁻ selectivities as high as 610, and these selectivities can be achieved without a diminution in flux relative to pure PAA/PAH membranes.

Such separations of ions of different valence are important in applications such as removal of harmful ions from water,[16−18] water softening,[19,20] production of edible salt from seawater,[21] and prevention of cooling water fouling.[22] Most of these applications require high permselectivity among different ions as well as high flux. Previous research on ion-exchange membranes

showed that permselectivity can be controlled by alteration of hydrophilicity/hydrophobicity,[23,24] cross-linking,[25,26] or surface charge density.[27] To achieve maximum efficiency in ion-separation processes, a minimal membrane thickness is also vital for achieving high flux. Multilayer polyelectrolyte films (MPFs) are attractive for ion separation membranes in part because of their minimal thickness.

Several studies on ion-exchange membranes already showed that monovalent/divalent ion selectivities can be greatly improved by adsorbing one layer of polyelectrolyte to the surface of the membrane.[27−29] However, even better permselectivities might be obtained when membranes are exclusively composed of MPFs. MPFs are versatile materials for separation membranes because both their thickness and surface charge density can, in principle, be controlled by varying deposition conditions such as pH,[30,31] salt concentration,[32−36] and the number of adsorbed layers.[37] Recent studies show that MPMs exhibit monovalent/divalent ion selectivities[3−5,15] that are at least partially due to Donnan exclusion at the charged surface layer of the polyelectrolyte films. Control over the charge density either at the surface or in the bulk of MPMs should thus yield control over membrane selectivity.

In this study, we use Cu²⁺-complexed PAA[38−40] to control the charge density within PAA/PAH films. Several groups recently showed that metallosupramolecular polyelectrolytes can be integrated into polyelectrolyte assemblies.[41−45] For example, Kurth and co-workers used iron-coordinated terpyridine as a polycation to form MPFs with poly(styrenesulfonate).[45] However, in the present case, we only partially complex PAA with Cu²⁺, so that PAA is still deposited as a polyanion. This allows the introduction of cation-exchange sites after removal of Cu²⁺ and the formation of highly selective membranes. Ion-transport studies and simple modeling of flux through these membranes suggest that selectivity is due to both Donnan exclusion and diffusional selectivity.

* To whom correspondence should be addressed: e-mail bruening@cem.msu.edu; phone (517) 355-9715 ext 237; Fax (517) 353−1793.
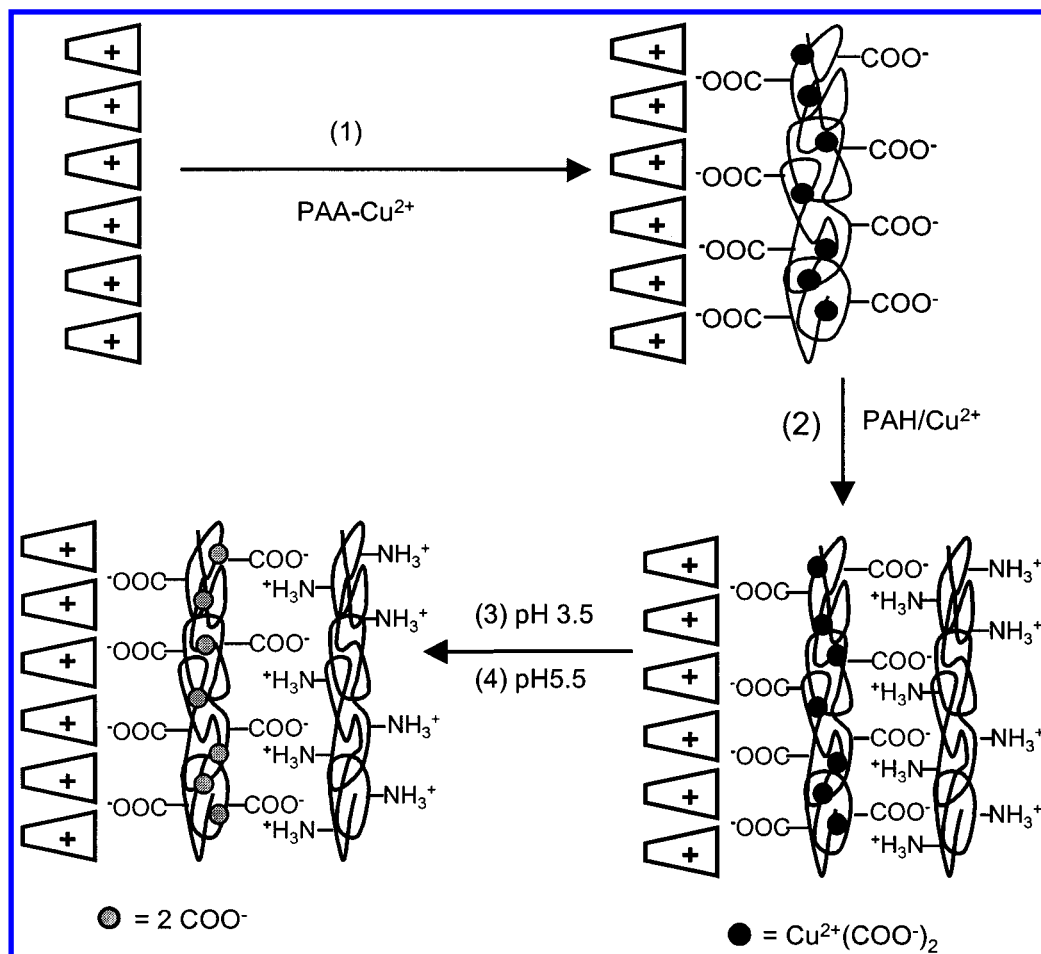
Figure 1. Preparation of Cu^{2+}-templated polyelectrolyte films on porous alumina supports. Step 1: adsorption of partially Cu^{2+}-complexed PAA on porous alumina. Step 2: adsorption of a polycation (PAH) in the presence of uncomplexed Cu^{2+}. Step 3: removal of Cu^{2+}. Step 4: deprotonation of the free carboxylic acid groups of PAA. Repetition of steps 1 and 2 produces multilayer films. Intertwining of layers is not shown for figure clarity.

Experimental Section

Chemicals and Solutions. Poly(allylamine hydrochloride) (PAH) ($M_w = 70\,000$), poly(acrylic acid) (PAA) ($M_w = 2000$), and 3-mercaptopropionic acid (MPA) were used as received from Aldrich. We used a relatively low molecular weight PAA to increase its solubility when complexed with Cu^{2+}. NaCl, $CuCl_2 \cdot 5H_2O$, and Na_2SO_4 were used as received from Spectrum. Anodisc porous alumina membranes with 0.02 μm diameter surface pores (Whatman Anodisc) were used as supports for deposition of polyelectrolyte films. For cross-linked PAA/PAH membranes, the outer polypropylene support ring of the alumina membrane was burned off prior to film deposition by heating at 400 °C for 18–20 h.[46,47] This was done in order to prevent melting of the polymer ring into the pores of the membrane during heat-induced cross-linking. Gold slides (200 nm of sputtered Au on 20 nm Cr on Si (100) wafers) were used as substrates for ellipsometric, external reflection FTIR spectroscopy, and electrochemical studies.

Film Preparation. Prior to film deposition, porous alumina substrates were cleaned in a UV/ozone cleaner (Boekel UV-Clean model 135500) for 15 min. Deposition of polyelectrolyte films began by dipping the substrate into a solution of PAA (0.04 M with respect to the repeating unit) containing $CuCl_2$ (2.5–7.5 mM) for 5 min followed by rinsing for 1 min with water (Milli-Q, 18 $M\Omega \cdot$cm). The substrate was then immersed in a solution of PAH (0.04 M with respect to the repeating unit and containing the same $CuCl_2$ concentration as PAA) for 5 min and rinsed with water for 1 min. The above procedure was repeated until the desired number of bilayers was deposited. The pH values of the deposition solutions were adjusted to 5.5, 6, or 6.6 using dilute HCl and NaOH solutions. Both PAH and PAA solutions contained 0.5 M NaCl as a supporting electrolyte in order to increase film thickness, and PAH and PAA depositions were always done at the same pH. The porous alumina membrane is asymmetric such that the permeate side contains 0.2 μm diameter pores, while pores on the filtrate side are 0.02 μm in diameter. Deposition of polyelectrolytes was limited to the filtrate side by using an O-ring holder. After deposition of the desired number of layers, membranes were rinsed well with water and dried with N_2. For cross-linking, membranes were placed in a flask that was purged with N_2 for 30 min and slowly heated to the desired temperature (~45 min ramping time). Then heating continued at the desired temperature (100–160 °C) for an additional 2 h under N_2 purging.

Similar to porous alumina supports, gold slides were UV cleaned prior to deposition. However, before polyelectrolyte adsorption, slides were immersed in an ethanolic solution of 2 mM MPA for 30 min and rinsed well with ethanol followed by deionized water (Milli-Q, 18 $M\Omega \cdot$cm). This produces a carboxylic acid-containing monolayer on the surface that will be charged upon deprotonation. We use MPA rather than a long chain alkanoic acid because the short chain thiols do not form compact monolayers and thus will not block electron transfer in electrochemical experiments.[48,49] The polyelectrolyte deposition procedure on gold was the same as for porous alumina, except that depositions started with PAH rather than PAA.

Film Characterization. Ellipsometry, external reflectance FTIR, and electrochemical measurements were performed as described previously.[15,50] The supporting electrolyte in all electrochemical experiments was 0.1 M Na_2SO_4. Before measuring cyclic voltammograms (scan rate of 0.1 V/s), solutions were purged with N_2 for 20–30 min. The exposed electrode area was 0.1 cm^2.

Ion-Transport Studies. Permeability studies were performed using two glass half cells as described in the preceding paper.[13] After every run the apparatus was washed well with water, and both cells were equilibrated with deionized water for 30 min before the next run. Alternating NaCl (pH 5.3) and Na$_2$SO$_4$ (pH 5.6) transport experiments were performed until two successive chloride fluxes matched within 10−15%. After the membrane achieved a steady Cl$^-$ flux value (this usually occurs after 4−5 alternate NaCl and Na$_2$SO$_4$ runs), it was removed from the permeability apparatus and dipped in pH 3.5 water (dilute HCl solution) for 1 h to ensure that all the copper was removed from the membrane. Then the membrane was immersed in deionized water (adjusted to pH 5−6 with a dilute NaOH solution) for 1−2 h to deprotonate the −COOH groups that were created upon removal of Cu^{2+}. Permeability experiments were then repeated, and Cl$^-$ fluxes differed by less than 5% when performed before and after a Na$_2$SO$_4$ permeability experiment. The Cl$^-$/SO$_4{}^{2-}$ selectivities and flux values reported here are calculated from permeability studies performed directly after immersing in pH 3.5 water followed by pH 5−6 water. The permeate cell conductivity values were converted to concentration using a calibration plot. Selectivity was obtained by dividing the slopes in plots of concentration vs time for different ions as described in the preceding paper.[13]

Results and Discussion

Synthesis and Characterization of Cu^{2+}-Templated PAA/PAH Films. Figure 1 shows schematically the preparation of Cu^{2+}-templated PAA/PAH films on porous alumina supports. The procedure begins by preparing PAA complexed with Cu^{2+}. To do this, we employ a PAA repeating unit to Cu^{2+} ratio of 8:1 so that ~25% of the −COO$^-$ groups of PAA will be complexed with Cu^{2+} (two −COO$^-$ groups should bind with one Cu^{2+}). The pH of the solution must be around 5.5 so that −COO$^-$ groups are mostly deprotonated and Cu(OH)$_2$ does not precipitate. Alternating adsorption of the Cu^{2+}-complexed PAA and PAH results in a MPF. Although UV/vis spectroscopy suggests that PAH does not form a complex with Cu^{2+} at pH 5.5,[51] we use the same Cu^{2+} concentration in PAH deposition as for PAA to prevent leaching of Cu^{2+} from the deposited PAA-Cu layer. After the desired number of layers are deposited, we expose films to a pH 3.5 solution to remove Cu^{2+} and create free −COOH groups on PAA chains. Subsequent immersion in a pH 5−6 solution deprotonates these −COOH groups and increases the fixed negative charge density in the film. The Cu^{2+}-templated PAA/PAH films differ from pure PAA/PAH films in that they contain −COO$^-$ groups that are not electrically compensated by the neighboring ammonium groups of PAH. For cross-linked films, the same deposition procedure (Figure 1) is followed, except the removal of Cu^{2+} and deprotonation of −COOH groups (steps 3 and 4 in Figure 1) occur after heating films for 2 h. Heating results in the formation of amide cross-links from −COO$^-$−NH$_3{}^+$ pairs.[14,52,53]

Cyclic voltammetry (Figure 2) of PAH/PAA-Cu films deposited on gold wafers confirms the presence of Cu^{2+} in these films as well as its removal at low pH. The peaks due to Cu^{2+}/Cu completely disappear after immersion of the electrode in pH 3.5 water (pH adjusted with 0.1 M HCl). Integration of the reduction or oxidation peak allows estimation of the amount of Cu^{2+} in the film, and this will prove useful in modeling of ion transport (vide infra). As a comparison, we also inserted Cu^{2+} into a 10-bilayer PAH/PAA film by immersing the film in a 0.1 M CuCl$_2$ solution for 20 h.[54] The amount of Cu^{2+} absorbed into this film was only about $^1/_7$ of the amount in a Cu^{2+}-templated film.
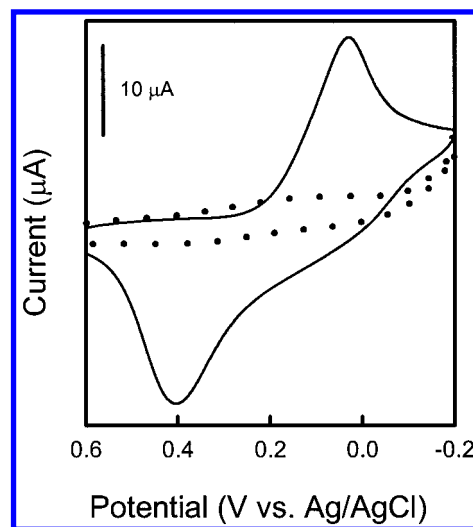

Figure 2. Cyclic voltammetry of a MPA-modified gold electrode coated with 10 bilayers of PAH/PAA-Cu before (solid line) and after exposing to pH 3.5 water (dotted line).
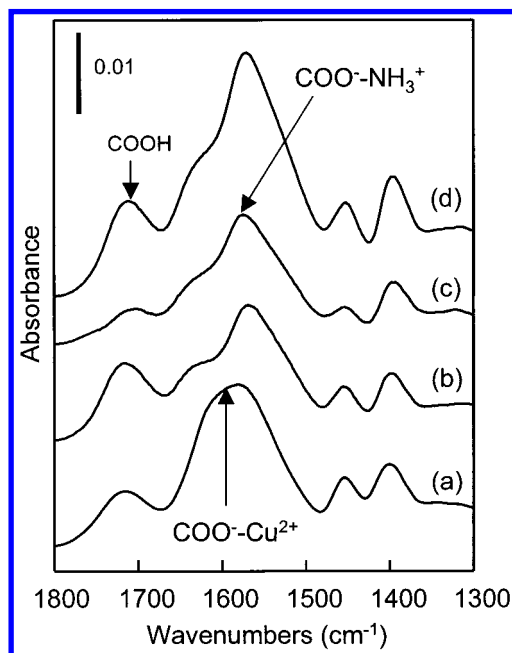

Figure 3. External reflectance FTIR spectra of (a) a 10-bilayer PAH/PAA-Cu film, (b) the same film after exposure to pH 3.5 water, (c) the film after exposure to pH 5−6 water, and (d) a 10-bilayer PAH/PAA film deposited without Cu^{2+}. All films were deposited on a gold wafer coated with a monolayer of MPA.

Reflectance FTIR spectra also confirm templating of PAH/PAA films with Cu^{2+}. The spectrum of a PAH/PAA-Cu film (spectrum a, Figure 3) shows a broadening of the −COO$^-$ symmetric stretch compared with the spectrum of a pure PAH/PAA film (spectrum d). This broadening results from counterion-induced changes in the energy of the −COO$^-$ stretch.[55] Upon exposure to pH 3.5 water and removal of Cu^{2+} (spectrum b, Figure 3), the −COO$^-$ symmetric stretch looks like that of a pure PAH/PAA film. Further, a 50% increase in the acid carbonyl peak (1715 cm^{-1}) after immersion in pH 3.5 water suggests formation of free −COOH groups from the Cu^{2+} complexes, as would be expected. Immersing the film in pH 5−6 water deprotonates −COOH groups and results in a decrease in the acid carbonyl peak (spectrum c, Figure 3).

Table 1. Anion Fluxes^a (mol cm^{-2} s^{-1}) through Bare Porous Alumina and Alumina Coated with PAA/PAH and PAA-Cu/ PAH Films Cross-Linked at Different Temperatures

film composition	cross-linking T (°C)	Cl$^-$ flux^a × 10^8	SO$_4{}^{2-}$ flux^a × 10^{11}	Cl$^-$/SO$_4{}^{2-}$ selectivity^c
bare		4.2 ± 0.1	3300 ± 200	1.3 ± 0.09
10 PAA/PAH		1.0 ± 0.2	1500 ± 300	0.7 ± 0.03
10 PAA-Cu/PAH^b		2.3 ± 0.3	270 ± 11	9 ± 1
10.5 PAA/PAH		1.3 ± 0.4	110 ± 50	13 ± 3
10.5 PAA-Cu/PAH^b		1.6 ± 0.2	30 ± 1	55 ± 3
10.5 PAA-Cu/PAH^b	100	1.6 ± 0.5	20 ± 4	80 ± 15
10.5 PAA-Cu/PAH^b	120	1.4 ± 0.2	6 ± 2	240 ± 80
10 PAA/PAH	130	0.09 ± 0.03	27 ± 5	3 ± 0.4
10 PAA-Cu/PAH^b	130	2.0 ± 0.06	32 ± 5	62 ± 11
10.5 PAA/PAH	130	0.07 ± 0.01	2.8 ± 0.9	26 ± 7
10.5 PAA-Cu/PAH^b	130	1.3 ± 0.05	2.1 ± 0.1	610 ± 20
10.5 PAA-Cu/PAH^b	140	0.51 ± 0.2	1.6 ± 0.5	330 ± 70
10.5 PAA-Cu/PAH^b	160	0.087 ± 0.04	3.0 ± 1	29 ± 1.3

^{a} Flux values were calculated from the slopes of plots of concentration in the receiving phase vs time. Errors represent standard deviations of measurements of at least three measurements. ^{b} Flux was measured after removal of Cu^{2+} from the membrane and deprotonation of newly formed −COOH groups. ^{c} Calculated as the average of selectivity values for each membrane and not from average flux values.
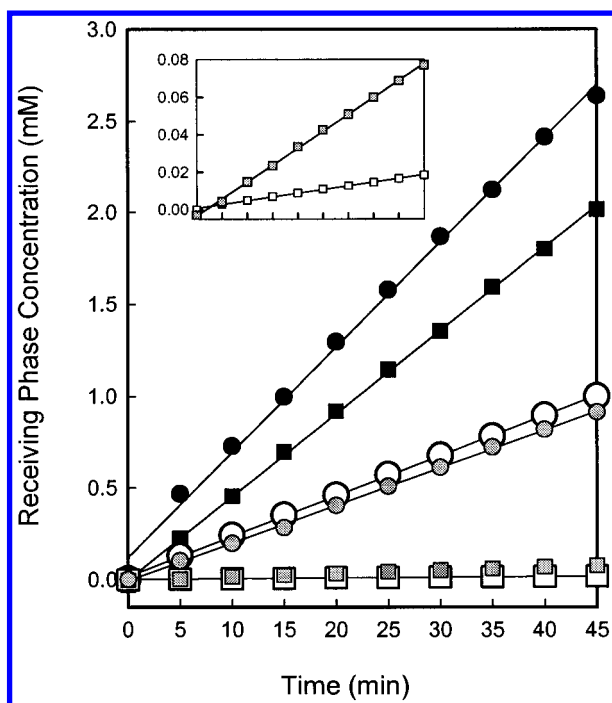

Figure 4. Receiving phase concentration as a function of time for a bare porous alumina membrane (black), an alumina membrane coated with 10.5 bilayers of Cu^{2+}-templated PAA/ PAH (open), and an alumina membrane coated with 10.5 bilayers of PAA/PAH (gray). Different symbols represent different salts: circles, NaCl; squares, Na$_2$SO$_4$. The inset shows SO$_4{}^{2-}$ concentration vs time for pure PAA/PAH (gray) and templated PAA/PAH (open). The membrane separates the receiving phase (initially deionized water) from a 0.1 M salt solution.

Anion Transport through Cu^{2+}-Templated PAA/ PAH Membranes. Ion-transport studies show that PAA-Cu/PAH membranes on porous alumina supports are significantly more selective than similar pure PAA/ PAH membranes. Figure 4 shows a plot of receiving-phase concentration as a function of time for membranes sandwiched between distilled water (receiving phase) and 0.1 M NaCl or Na$_2$SO$_4$ (source phase). These plots show that the Cl$^-$ flux through both Cu^{2+}-templated and pure PAA/PAH membranes is 30−40% of that through bare porous alumina. However, 10.5-bilayer PAA-Cu/ PAH membranes (the top layer in the film is PAA-Cu) show a 4-fold decrease in SO$_4{}^{2-}$ flux relative to pure 10.5-bilayer PAA/PAH membranes as shown in the inset

of Figure 4. Overall, Cl$^-$/SO$_4{}^{2-}$ selectivity increases 4-fold due to templating (Table 1).

Cross-Linked Cu^{2+}-Templated PAA/PAH Membranes. One possible limitation to Cl$^-$/SO$_4{}^{2-}$ selectivity is that swelling in water may decrease charge density, reducing Donnan exclusion of SO$_4{}^{2-}$ and decreasing selectivity. In an effort to limit film swelling, we cross-linked PAA-Cu/PAH films by heating under N$_2$ to form amide bonds through reaction of the ammonium groups of PAH and the uncomplexed carboxylate groups of PAA. Reflectance FTIR spectroscopy confirms that the cross-linking reaction occurs.[14] After heating at 160 °C, external reflectance FTIR spectra show a large reduction in the intensity of −COO$^-$ peaks at 1570 and 1400 cm^{-1} and the appearance of amide peaks at 1660 and 1550 cm^{-1} (Supporting Information, Figure 1). At lower heating temperatures, the amide peaks are more clearly visible after exposing the cross-linked films to low-pH solutions because peaks due to Cu^{2+}−COO$^-$ complexes also appear in this region of the spectrum. The degree of cross-linking depends greatly on heating temperature as indicated by amide peaks that increase with cross-linking temperature.[14]

Diffusion dialysis studies show that as cross-linking temperature increases, Cl$^-$/SO$_4{}^{2-}$ selectivity increases and then peaks when cross-linking at 130 °C (Table 1, 10.5-bilayer PAA-Cu/PAH films). Partially cross-linked 10.5-bilayer PAA-Cu/PAH membranes (130 °C) show a 10-fold increase in Cl$^-$/SO$_4{}^{2-}$ selectivity over unheated, templated membranes, and this increase is achieved with only a 20% decrease in Cl$^-$ flux. At higher cross-linking temperatures, Cl$^-$ flux begins to drop dramatically, presumably due to a tighter membrane structure. Sulfate flux does not continue to drop significantly at higher cross-linking temperatures, and thus Cl$^-$/SO$_4{}^{2-}$ selectivity eventually decreases.

Compared with pure PAA/PAH membranes, the selectivities and fluxes through partially cross-linked PAA-Cu/PAH membranes are remarkable. Table 1 shows that partially cross-linked (130 °C) 10.5-bilayer PAA-Cu/PAH membranes show a 20-fold increase in Cl$^-$/SO$_4{}^{2-}$ selectivity relative to similar cross-linked pure PAA/PAH membranes. Additionally, the Cl$^-$ flux through these cross-linked Cu^{2+}-templated membranes is 20-fold higher than the Cl$^-$ flux through pure PAA/ PAH membranes cross-linked at the same temperature. This may be due to the formation of new transport

Table 2. Thicknesses, Fluxes (mol cm^{-2} s^{-1}) and Cu^{2+} Concentrations (M) in Partially Cross-Linked, 10.5-Bilayer PAA-Cu/PAH Films Deposited at Different pH Values

deposit-ion pH[a]	Cu^{2+} concn[b]	Cl$^-$ flux[c] $\times 10^8$	SO$_4{}^{2-}$ flux[c] $\times 10^{11}$	Cl$^-$/SO$_4{}^{2-}$ selectivity[d]	thick-ness[e] (Å)
5.5	1.0 ± 0.06	1.3 ± 0.05	2.1 ± 0.1	610 ± 20	170 ± 3
6	0.9 ± 0.04	1.1 ± 0.2	2.6 ± 0.4	430 ± 90	170 ± 6
6.6	0.3 ± 0.1	1.6 ± 0.3	170 ± 42	11 ± 4	170 ± 10

[a] Both PAA-Cu and PAH were deposited at this pH. [b] Cu^{2+} concentration in the membrane was estimated from the area of the reduction peak in a cyclic voltammagram of a film on gold. The area was converted to number of moles of Cu^{2+}/cm^2, and this value was divided by the ellipsometric film thickness to obtain the concentration. [c] Error values represent standard deviations. [d] Calculated as the average of selectivity values for each membrane and not from average flux values. [e] Thicknesses are for 10-bilayer PAH/PAA-Cu films deposited on gold wafers as described in the Experimental Section.

pathways upon removal of Cu^{2+} or a lower degree of cross-linking in the templated film.

Changing the Surface Charge of Membranes. Our previous studies[5,15] of MPMs showed that much of the ion-transport selectivity in these systems is due to a high charge density at the membrane surface. However, Cu^{2+}-templated membranes differ from previous MPMs in that they contain fixed charge throughout the membrane. In an effort to understand more about selectivities in PAA-Cu/PAH membranes, we changed the terminating layer of these films from PAA to positively charged PAH. If selectivity in these systems is largely due to charge at their surface, changing the outer layer from a polyanion to a polycation should have a dramatic effect on ion transport.

Changing the surface from PAA-Cu (10.5-bilayer films) to PAH (10-bilayer films) in cross-linked (130 °C), templated films resulted in a 15-fold increase in SO$_4{}^{2-}$ flux and a 50% increase in Cl$^-$ flux (Table 1). Thus, Cl$^-$/SO$_4{}^{2-}$ selectivity decreased from 610 to 60 on going from a 10.5-bilayer to a 10-bilayer cross-linked PAA-Cu/PAH film. In the case of unheated Cu^{2+}-templated membranes, terminating with PAH rather than PAA-Cu^{2+} yielded a decrease in Cl$^-$/SO$_4{}^{2-}$ selectivity from 55 to 9. These data clearly indicate that Donnan exclusion at the film surface plays a large role in determining selectivity. For unheated, pure PAA/PAH membranes, Cl$^-$/SO$_4{}^{2-}$ selectivity actually reverses (from 13 to 0.7) upon changing the top layer from PAA to PAH.[56] In contrast, with Cu^{2+}-templated films we still see a significant Cl$^-$/SO$_4{}^{2-}$ selectivity when the surface of the membrane is positively charged because of the fixed negative charge density in the bulk of the membrane.

Anion Transport through Partially Cross-Linked, Cu^{2+}-Templated Membranes Deposited at Different pH Values. Variation of the pH at which PAA-Cu/PAH films are deposited allows some control over the amount of Cu^{2+} in these films and may provide a means for controlling transport selectivity. Table 2 gives the Cl$^-$/SO$_4{}^{2-}$ selectivity values for partially cross-linked 10.5-bilayer PAA-Cu/PAH membranes deposited from solutions at three different pH values (5.5, 6, and 6.6). We also tried to deposit membranes at pH values <5.5, but under these conditions, polymer precipitates from deposion solutions. Selectivity is highest for films deposited at pH 5.5 and decreases at higher deposition pH values. The ellipsometric thicknesses (Table 2) of similar films on gold-coated wafers are independent of
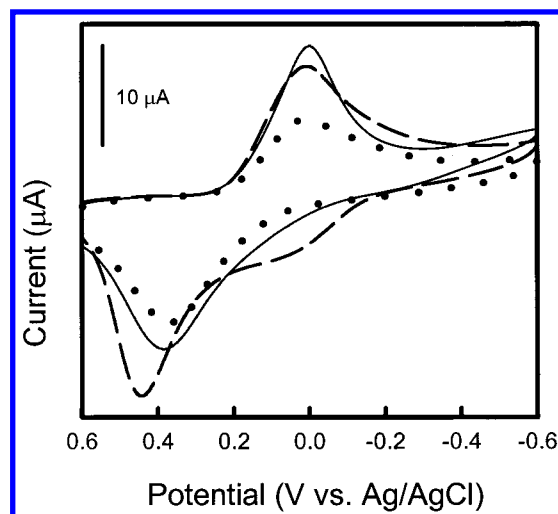

Figure 5. Cyclic voltammetry of 10-bilayer films of PAH/PAA-Cu^{2+} deposited at different deposition pH values on MPA-modified gold surfaces: pH 5.5, dashed line; pH 6, solid line; pH 6.6, dotted line. Areas of the reduction peaks were calculated by drawing the baseline from the current value at a potential of 0.3 V to the current value at −0.5 V.

pH[57] over this range of values, so selectivity differences are likely due to changes in charge density. The UV/vis spectra of the PAH/Cu^{2+} solutions showed a shift in the Cu^{2+} absorption peak from 820 nm at pH 5.5 to 780 nm at pH 6 and to 710 nm at pH 6.6, suggesting that the amine groups of PAH begin to form complexes with Cu^{2+} at the higher pH values. In addition, at higher pH values Cu^{2+} can form hydroxide complexes. These competing reactions probably reduce the amount of Cu^{2+} deposited in the membrane as −COO$^-$−Cu^{2+} complexes.

To quantitatively investigate fixed-charge density in PAH/PAA-Cu films, we employed cyclic voltammetry (Figure 5). By integrating the area of the reduction peak, Cu^{2+} concentrations within the film can be estimated. In agreement with transport studies, Table 2 shows that the maximum amount of copper is deposited at pH 5.5. Hence, after removal of Cu^{2+} from the film, higher charge densities should enhance Cl$^-$/SO$_4{}^{2-}$ selectivity for films deposited at the lower pH values.

Anion Transport through Partially Cross-Linked, Cu^{2+}-Templated Membranes Deposited with Different Cu^{2+} Concentrations. Altering the amount of Cu^{2+} present during deposition should provide another means for controlling fixed charge and selectivity in membranes. We chose to do these studies at pH 6, because at pH 5.5, higher Cu^{2+} concentrations resulted in precipitation. We employed Cu^{2+} concentrations of 2.5, 5, or 7.5 mM in both PAA and PAH solutions, and membranes were cross-linked at 130 °C after deposition. Table 3 gives the Cl$^-$/SO$_4{}^{2-}$ selectivities and flux values for these membranes.

Cl$^-$/SO$_4{}^{2-}$ selectivity was highest when the concentration of Cu^{2+} present during deposition was 5 mM. Cyclic voltammetry (Supporting Information, Figure 2) and ellipsometric data (Table 3) for analogous films deposited on gold wafers indicate that the highest Cu^{2+} concentration occurs in films deposited with 5 mM Cu^{2+}. This happens because film thickness increases greatly when the Cu^{2+} concentration during deposition is 7.5 mM. Hence, the highest selectivity is observed for the MPMs deposited in the presence of 5 mM Cu^{2+}. The structure of films may also depend on the Cu^{2+} concentration present during deposition.[58,59] This might ex-

Table 3. Anion Fluxes (mol cm^{-2} s^{-1}), Thicknesses, and Estimated Cu^{2+} Concentrations (M) in Partially Cross-Linked (130 °C) 10.5-Bilayer PAA-Cu/PAH Membranes and Films Deposited Using Different Cu^{2+} Concentrations

Cu^{2+} concn used in deposition[a] (mM)	Cl$^-$ flux × 10^8	SO$_4^{2-}$ flux × 10^{11}	Cl$^-$/SO$_4^{2-}$ selectivity[b]	estimated Cu^{2+} concn[c]	thickness[d] (Å)
0	0.056 ± 0.01	5 ± 2	11 ± 2	0	177 ± 26
2.5	1.5 ± 0.1	19 ± 2	81 ± 3	0.3 ± 0.01	204 ± 9
5.0	1.1 ± 0.2	2.6 ± 0.4	430 ± 90	1.0 ± 0.06	170 ± 6
7.5	2.5 ± 0.3	71 ± 15	41 ± 11	0.6 ± 0.04	316 ± 14

[a] Both PAA and PAH deposition solutions contained the same concentration of Cu^{2+} and had a pH of 6. [b] Calculated as the average of selectivity values for each membrane and not from average flux values. [c] Cu^{2+} concentration was determined using cyclic voltammetry before cross-linking and ellipsometric thicknesses measured after cross-linking. [d] Thicknesses reported are those for 10-bilayer PAH/PAA-Cu films on gold wafer after cross-linking at 130 °C for 2 h as described in the Experimental Section.

Table 4. Diffusion Coefficients Obtained from Modeling Ion Transport through 10.5-Bilayer PAA-Cu^{2+}/PAH Membranes Cross-Linked at Different Temperatures

cross-linking temp (°C)	Cl$^-$ diffusion coeff (cm^2 s^{-1})	SO$_4^{2-}$ diffusion coeff (cm^2 s^{-1})	bulk fixed charge density[a] (mol/cm^3)	estimated surface fixed charge density[65] (mol/cm^3)	diffusional selectivity[b]	electrostatic exclusion selectivity[c]
unheated	8.8 × 10^{-9}	1.4 × 10^{-9}	1.4 × 10^{-3}	1.1 × 10^{-2}	6	9
100	8.8 × 10^{-9}	1.1 × 10^{-9}	1.5 × 10^{-3}	1.2 × 10^{-2}	8	10
120	7.4 × 10^{-9}	3.6 × 10^{-10}	1.6 × 10^{-3}	1.3 × 10^{-2}	20.5	11.7
130	6.8 × 10^{-9}	1.5 × 10^{-10}	2.0 × 10^{-3}	1.6 × 10^{-2}	45	13.6
140	2.4 × 10^{-9}	1.1 × 10^{-10}	1.9 × 10^{-3}	1.5 × 10^{-2}	22	15
160	4.1 × 10^{-10}	2.2 × 10^{-10}	2.1 × 10^{-3}	1.7 × 10^{-2}	1.7	17

[a] Determined using cyclic voltammetry and ellipsometry. [b] The diffusional selectivity is the ratio of diffusion coefficients obtained from the model. [c] Total Cl$^-$/SO$_4^{2-}$ selectivity divided by diffusional selectivity.

plain why films deposited with 7.5 mM Cu^{2+} are less selective than films deposited with 2.5 mM Cu^{2+} even though the former films have a higher concentration of Cu^{2+}.

Modeling of Anion Transport through Cu^{2+}-Templated PAA/PAH Membranes. To better understand the observed selectivities and fluxes through templated membranes, we began developing a simple model for ion transport based on previous models of ion-exchange membranes[60,61] and MPMs.[62] This model is identical to that presented in the preceding paper,[13] except that we employ a two-layer model of the MPF, assuming the bulk of the membrane as one layer and the surface as another (Figure 6). The charge density in these two regions should be different as several recent studies[63,64] show that net fixed charge in standard MPFs resides primarily at the surface. However, in templated films, removal of Cu^{2+} yields ion-exchange sites in the bulk of the membrane as well as on the surface. We estimated the fixed negative charge density in the bulk from the amount of Cu^{2+} determined from cyclic voltammetry (noting that every Cu^{2+} binds with two COO$^-$ groups) and from the ellipsometric thicknesses of corresponding films deposited on gold. To estimate surface charge density, we assumed that this layer was composed of pure PAA.[65]

With a simplified structural model in hand, we simulated diffusion coefficients in these templated films as described in the preceding paper. The diffusion coefficients determined for Cl$^-$ and SO$_4^{2-}$ are listed in Table 4. These calculations on unheated, templated membranes yielded Cl$^-$ diffusion coefficients on the order of 10^{-8} cm^2/s, and the Cl$^-$ diffusion coefficient was a factor of 6 higher than that of SO$_4^{2-}$. Miyoshi reported[60] that effective diffusion coefficients through ion-exchange membranes are as low as 10^{-7} to ~10^{-8} cm^2/s for Na$^+$ and Mg^{2+}, reasonably close to the Cl$^-$ values we calculate. The calculated diffusion coefficients suggest that selectivity is about equally due to Donnan exclusion and diffusivity differences, as the measured selectivity is the product of diffusive and partition selectivities.
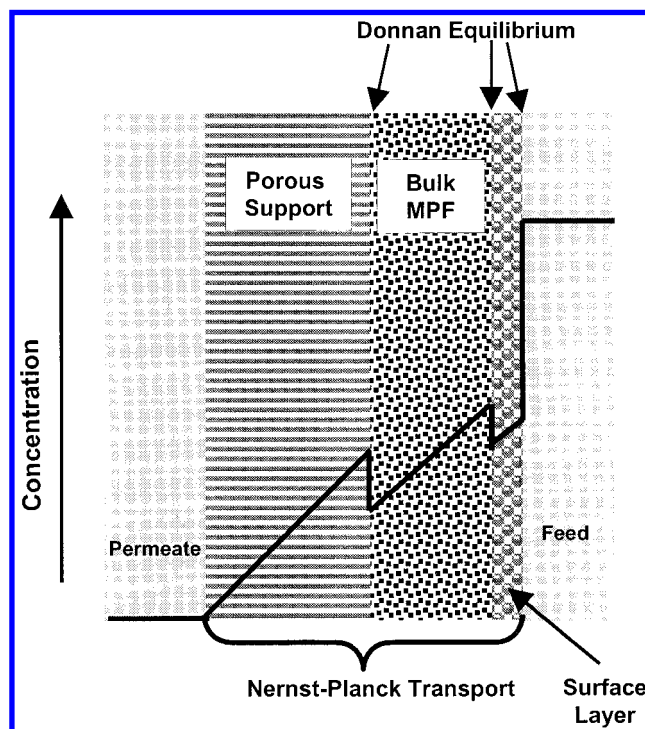

Figure 6. Schematic representation of the model used to simulate the transport through templated MPMs. The membrane consists of two charged layers, a surface layer, and the membrane bulk. The line represents a hypothetical concentration profile for the excluded ion.

Modeling studies on cross-linked, templated membranes show that as the cross-linking temperature increases, diffusion coefficients generally decrease (Table 4). This is reasonable because cross-linking reduces swelling and hence free volume. At low cross-linking temperatures, decreases in the SO$_4^{2-}$ diffusion coefficient are more dramatic than those for Cl$^-$, and this may be due to size exclusion or hydrophobicity effects.[23,66,67] At 160 °C, the diffusion coefficient of SO$_4^{2-}$ actually increased, probably because fixed charge den-

sity decreased at this cross-linking temperature, and we could not take this into account. At a cross-linking temperature of 130 °C, the calculated Cl^- diffusion coefficient was 45-fold higher than that of SO_4^{2-}. These simple calculations suggest that the highest selectivities in cross-linked films are due to both diffusion and Donnan selectivities. We should note, however, that this model does not take into account activity coefficients or the effect of hydrophobicity on partitioning. Several previous studies also showed that diffusion through charged membranes can be complicated due to electrostatic interactions.[68,69] Additionally, charge distributions are oversimplified and only approximate. However, the modeling studies do strongly indicate that selectivity is only partly due to Donnan exclusion. A full understanding of transport through MPMs will likely require measurement of diffusion and partition coefficients.

Conclusions

Partial complexation of the $-COO^-$ groups of PAA with Cu^{2+} provides a convenient method to enhance fixed negative charge density in MPMs. Removal of the Cu^{2+} leaves behind $-COOH$ groups that behaves as ion-exchange sites. Diffusion dialysis studies with Cu^{2+}-templated membranes show that templating increases Cl^-/SO_4^{2-} selectivities. Postdeposition cross-linking of these membranes further enhances Cl^-/SO_4^{2-} selectivities to values as high as 610. Changing the capping polymer from negatively charged PAA to positively charged PAH greatly reduces Cl^-/SO_4^{2-} selectivity, showing that selectivity is highly dependent on surface charge. Modeling of ion transport data using a simple two-layer model of MPFs suggests that the observed Cl^-/SO_4^{2-} selectivities are due to both Donnan exclusion and differences in diffusivities of ions.

Supporting Information Available: FTIR spectra of 10-bilayer PAH/PAA-Cu films before and after cross-linking at 160 °C and cyclic voltammetry of 10-bilayer PAH/PAA-Cu films deposited at different Cu^{2+} concentrations. This material is available free of charge via the Internet at http://pubs.acs.org.

References and Notes

(1) Decher, G. *Science* **1997**, *277*, 1232−1237.
(2) Decher, G.; Hong, J. D. *Ber. Bunsen-Ges. Phys. Chem.* **1991**, *95*, 1430−1434.
(3) Krasemann, L.; Tieke, B. *Mater. Sci. Eng. C* **1999**, *8−9*, 513−518.
(4) Krasemann, L.; Tieke, B. *Langmuir* **2000**, *16*, 287−290.
(5) Harris, J. J.; Stair, J. L.; Bruening, M. L. *Chem. Mater.* **2000**, *12*, 1941−1947.
(6) Leväsalmi, J.-M.; McCarthy, T. J. *Macromolecules* **1997**, *30*, 1752−1757.
(7) Stroeve, P.; Vasquez, V.; Coelho, M. A. N.; Rabolt, J. F. *Thin Solid Films* **1996**, *285*, 708−712.
(8) Kotov, N. A.; Magonou, S.; Tropsha, E. *Chem. Mater.* **1998**, *10*, 886−895.
(9) van Ackern, F.; Krasemann, L.; Tieke, B. *Thin Solid Films* **1998**, *329*, 762−766.
(10) Krasemann, L.; Tieke, B. *Chem. Eng. Technol.* **2000**, *23*, 211−213.
(11) Krasemann, L.; Tieke, B. *J. Membr. Sci.* **1998**, *150*, 23−30.
(12) Meier-Haack, J.; Lenk, W.; Lehmann, D.; Lunkwitz, K. *J. Membr. Sci.* **2001**, *184*, 233−243.
(13) Dai, J.; Balachandra, A. M.; Lee, J. I.; Bruening, M. L. *Macromolecules* **2002**, *35*, 3164−3170.
(14) Harris, J. J.; DeRose, P. M.; Bruening, M. L. *J. Am. Chem. Soc.* **1999**, *121*, 1978−1979.
(15) Stair, J. L.; Harris, J. J.; Bruening, M. L. *Chem. Mater.* **2001**, *13*, 2641−2648.
(16) Hell, F.; Lahnsteiner, J.; Frischherz, H.; Baumgartner, G. *Desalination* **1998**, *117*, 173−180.
(17) Amor, Z.; Bariou, B.; Mameri, N.; Taky, M.; Nicolas, S.; Elmidaoui, A. *Desalination* **2001**, *133*, 215−223.
(18) Sata, T.; Yamaguchi, T.; Matsusaki, K. *J. Chem. Soc., Chem. Commun.* **1995**, *11*, 1153−1154.
(19) Mika, A. M.; Childs, R. F.; Dickson, J. M. *Desalination* **1999**, *121*, 149−158.
(20) Brett, S. W.; Gaterell, M. R.; Morse, G. K.; Lester, J. N. *Environ. Technol.* **1999**, *20*, 1009−1018.
(21) Takata, K.; Yamamoto, Y.; Sata, T. *Bull. Chem. Soc. Jpn.* **1996**, *69*, 797−804.
(22) Bader, M. S. H. *J. Hazard Mater.* **2000**, *B73*, 269−283.
(23) Sata, T.; Mine, K.; Higa, M. *J. Membr. Sci.* **1998**, *141*, 137−144.
(24) Sata, T.; Mine, K.; Tagami, Y.; Higa, M.; Matsusaki, K. *J. Chem. Soc., Faraday Trans.* **1998**, *94*, 147−153.
(25) Sata, T.; Nojima, S. *J. Polym. Sci., Polym. Phys. Ed.* **1999**, *37*, 1773−1785.
(26) Sata, T.; Emori, S. I.; Matsusaki, K. *J. Polym. Sci., Polym. Phys. Ed.* **1999**, *37*, 793- 804.
(27) Matsusaki, K.; Hashimoto, N.; Kuroki, M.; Sata, T. *Anal. Sci.* **1997**, *13*, 345−349.
(28) Tsuru, T.; Nakao, S.-I.; Kimura, S. *J. Membr. Sci.* **1995**, *108*, 269−278.
(29) Urairi, M.; Tsuru, T.; Nakao, S.; Kimura, S. *J. Membr. Sci.* **1992**, *70*, 153−162.
(30) Yoo, D.; Shiratori, S. S.; Rubner, M. F. *Macromolecules* **1998**, *31*, 4309−4318.
(31) Shiratori, S. S.; Rubner, M. F. *Macromolecules* **2000**, *33*, 4213−4219.
(32) Sukhorukov, G. B.; Schmitt, J.; Decher, G. *Ber. Bunsen-Ges. Phys. Chem.* **1996**, *100*, 948−953.
(33) Sukhishvili, S. A.; Granick, S. *J. Chem. Phys.* **1998**, *109*, 6861−6868.
(34) Dubas, S. T.; Schlenoff, J. B. *Macromolecules* **1999**, *32*, 8153−8160.
(35) Losche, M.; Schmitt, J.; Decher, G.; Bouwman, W. G.; Kjaer, K. *Macromolecules* **1998**, *31*, 8893−8906.
(36) Lvov, Y.; Decher, G.; Möhwald, H. *Langmuir* **1993**, *9*, 481−486.
(37) Decher, G.; Hong, J. D.; Schmitt, J. *Thin Solid Films* **1992**, *210/211*, 831−835.
(38) Gotoh, Y.; Igarashi, R.; Ohkoshi, Y.; Nagura, M.; Akamatsu, K.; Deki, S. *J. Mater. Chem.* **2000**, *10*, 2548−2552.
(39) Rivas, B. L.; Schiappacasse, N.; Basaez, L. A. *Polym. Bull. (Berlin)* **2000**, *45*, 259−265.
(40) Porasso, R. D.; Benegas, J. C.; Hoop, M. A. G. T. v. d. *J. Phys. Chem. B* **1999**, *103*, 2361−2365.
(41) Kurth, D. G.; Osterhout, R. *Langmuir* **1999**, *15*, 4842−4846.
(42) Caruso, F.; Schuler, C.; Kurth, D. G. *Chem. Mater.* **1999**, *11*, 3394−3399.
(43) Xiong, H.; Cheng, M.; Zhou, Z.; Zhang, X.; Shen, J. *Adv. Mater.* **1998**, *10*, 529−532.
(44) Zhang, X.; Shen, J. C. *Adv. Mater.* **1999**, *11*, 1139−1143.
(45) Schütte, M.; Kurth, D. G.; Linford, M. R.; Cölfen, H.; Möhwald, H. *Angew. Chem., Int. Ed.* **1998**, *37*, 2891−2893.
(46) Chen, W. J.; Martin, C. R. *J. Membr. Sci.* **1995**, *104*, 101−108.
(47) Chen, W. J.; Aranda, P.; Martin, C. R. *J. Membr. Sci.* **1995**, *107*, 199−207.
(48) Dai, Z.; Ju, H. *Phys. Chem. Chem. Phys.* **2001**, *3*, 3769−3773.
(49) Bain, C. D.; Troughton, E. B.; Tao, Y. T.; Evall, J.; Whitesides, G. M.; Nuzzo, R. G. *J. Am. Chem. Soc.* **1989**, *111*, 321−335.
(50) Harris, J. J.; Bruening, M. L. *Langmuir* **2000**, *16*, 2006−2013.
(51) At pH 5.5, the UV/vis spectrum of PAH/ Cu^{2+} solutions is identical to that of a $CuCl_2$ solution containing the same Cu^{2+} concentration.
(52) Dai, J.; Sullivan, D. M.; Bruening, M. L. *Ind. Eng. Chem. Res.* **2000**, *39*, 3528−3535.
(53) Dai, J.; Jensen, A. W.; Mohanty, D. K.; Erndt, J.; Bruening, M. L. *Langmuir* **2001**, *17*, 931−937.
(54) Joly, S.; Kane, R.; Radzilowski, L.; Wang, T.; Wu, A.; Cohen, R. E.; Thomas, E. L.; Rubner, M. F. *Langmuir* **2000**, *16*, 1354−1359.
(55) Deacon, G. B.; Phillips, R. J. *Coord. Chem. Rev.* **1980**, *33*, 227−250.

(56) Because films were prepared in the presence of 0.5 M NaCl, effects of surface charge are much more pronounced in this work than in the preceding paper.

(57) Rubner and co-workers reported that the thickness of similar MPF's are dependent on deposition pH (reference 31). However, in our case we use a supporting electrolyte (NaCl) and Cu^{2+} in the deposition solution.

(58) Mendelsohn, J. D.; Barrett, C. J.; Chan, V. V.; Pal, A. J.; Mayes, A. M.; Rubner, M. F. *Langmuir* **2000**, *16*, 5017−5023.

(59) Fery, A.; Schöler, B.; Cassagneau, T.; Caruso, F. *Langmuir* **2001**, *17*, 3779−3783.

(60) Miyoshi, H. *J. Membr. Sci.* **1998**, *141*, 101−110.

(61) Manzanares, J. A.; Mafé, S.; Pellicer, J. *J. Phys. Chem.* **1991**, *95*, 5620−5624.

(62) Lebedev, K.; Ramirez, P.; Mafé, S.; Pellicer, J. *Langmuir* **2000**, *16*, 9941−9943.

(63) Lowack, K.; Helm, C. A. *Macromolecules* **1998**, *31*, 823−833.

(64) Schlenoff, J. B.; Ly, H.; Li, M. *J. Am. Chem. Soc.* **1998**, *120*, 7626−7634.

(65) To estimate the charge density in the surface layer, we first determined the concentration of Cu^{2+} in a 10-bilayer film using cyclic voltammetry and ellipsometry and then multiplied this value by a factor of 8 to get the $-COO^-/-COOH$ concentration in the film. We multiplied this value by a factor of 2 because the surface of the film is mostly PAA rather than PAH/PAA. We assumed that $-COOH$ groups were completely deprotonated.

(66) Sata, T. *J. Membr. Sci.* **1994**, *93*, 117−135.

(67) Sata, T.; Yamaguchi, T.; Matsusaki, K. *J. Phys. Chem.* **1995**, *99*, 12875−12882.

(68) Beerlage, M. A. M.; Peeters, J. M. M.; Nolten, J. A. M.; Mulder, M. H. V.; Strathmann, H. *J. Appl. Polym. Sci.* **2000**, *75*, 1180−1193.

(69) Robertson, B. C.; Zydney, A. L. *J. Membr. Sci.* **1990**, *49*, 287−303.